Temperature effects on supercontinuum generation using a continuous-wave Raman fiber laser

S. Martin-Lopez [*,a], M. Gonzalez-Herraez [a,b], P. Corredera [a], M. L. Hernanz [a], A. Carrasco [a], and J. A. Mendez [a]

[a] *Instituto de Fisica Aplicada, CSIC. Serrano 144, 28006 Madrid.*

[b] *Departamento de Electronica, Escuela Politecnica Superior, Universidad de Alcala. Campus Universitario, 28871, Alcala de Henares, Madrid*

Abstract

We describe the effect of temperature variations on supercontinuum (SC) generation in optical fibers using a continuous-wave (CW) Raman fiber laser as a pump. We achieve supercontinuum generation by pumping only ∼2 W of power into a 7 km-long nonzero dispersion-shifted fiber (NZDSF) in the region of small anomalous dispersion. In these conditions, the supercontinuum builds up basically on modulational instability and Raman. At room temperature, the supercontinuum covers effectively the S, C and L transmission bands defined by the International Telecommunication Union (ITU). Temperature tuning of the fiber environment provides a means of tuning the fiber dispersion, and thus a means of changing the width and shape of the supercontinuum spectrum. We demonstrate a 27% increase in the 10-dB SC width. We believe that the application of this new tuning mechanism to other experimental configurations using pulsed sources might be used to produce extremely broad supercontinuums.

Key words: supercontinuum, Raman scattering, modulational instability, temperature dependence

PACS: 42.65.Dr, 42.79.Sz, 42.81.Dp, 42.72.Ai

1 Introduction

Supercontinuum (SC) generation in optical fibers and waveguides has attracted considerable research interest in the last years [1-12] Applications of supercontinuum generation in optical fibers can be found in fields such as optical frequency metrology [1,2] optical coherence tomography [3,4] and multiple optical carrier generation for wavelength-division multiplexing [5,6]. Most of the experiments performed up to date have been performed using nanosecond or picosecond pulses of high peak power and/or specialty fibers such as photonic crystal fibers [7] or dispersion-tapered fibers [8]. Supercontinuum generation using continuous-wave (CW) sources was demonstrated only recently [9,10,11]. In the case of a CW pump, long fibers are needed to initiate the SC since the typical power of the CW sources goes only up to a few watts and longer interaction lengths are required. In a previous work [11] we demonstrated the possibility to generate a broad SC using a 7-km long conventional nonzero dispersion-shifted fiber pumped by a Raman fiber laser (RFL) tuned to the region of small anomalous dispersion of the fiber. The output SC had a 20-dB width of over 200 nm, covering the S, C and L transmission bands defined by the International Telecommunication Union (ITU). We showed that such a source could be used to perform highly accu-

* To whom correspondence should be addressed
Email address: ltqm358@cetef.csic.es (S. Martin-Lopez).

rate characterization of polarization-mode dispersion in very long (> 200 km) fiber links. In this Letter we demonstrate experimentally that by changing the temperature of the fiber environment we can optimize the width and flatness of the generated SC. We believe that this idea might have important implications towards the development of efficient supercontinuum sources with high power spectral density at arbitrary pump wavelengths.

2 Experiment

Supercontinuum generation in optical fiber is generally caused by the combined effect of self-phase modulation (SPM), modulational instability (MI) and stimulated Raman scattering (SRS). **In principle,**in our case, the effect of self-phase modulation is basically negligible since the pump is CW. Thus, our continuum **should be** mainly caused by modulational instability and Raman. These processes are both stimulated, and so they can be thought of as initially seeded by pump laser noise [10]. **But our CW pump laser is partially coherent and some intensity fluctuations are present in the pump. These intensity oscillations are amplified due to MI [13,14].** Efficient generation of a broad modulational instability spectrum can only be achieved in the region of very small anomalous dispersion ($D > 0$ or $\beta_2 < 0$). The use of a long fiber with low loss ensures strong power transfer from pump to MI and a low SRS threshold (∼1 W). In these conditions, SC generation is possible with low peak power sources (and even CW as in this case) while allowing strong pump depletion and high power densities [12] (in the order of mW/nm in our case).

The pump used in our experiment was a continuous-wave Cascaded Raman

Fiber Laser (C-RFL) with a single-mode output tuned at 1455.3 nm, and whose spectrum has been detailed elsewhere [11]. The laser output is depolarized and the maximum output power reaches 2.1 W. A feedback control ensures that the output power of the RFL remains constant and controlled with an accuracy of ±10 mW. The line width of the RFL grows as the power is increased. For a pump power of 2.1 W, the full width at half maximum (FWHM) of the laser output is 1.1 nm, with a RIN < -110 dBc/Hz (measured in the range 0-1 GHz). We use a 7-km-long spool of nonzero dispersion-shifted fiber with an expected dispersion at the wavelength of the pump of 0.081 ps·nm^{-1}·km^{-1}. The dispersion slope at this wavelength is 0.045 ps·nm^{-2}·km^{-1}. The uniformity of the chromatic dispersion along the fiber was measured using a method developed by some of us [16] and was found to be better than ±0.1 ps·nm^{-1}·km^{-1} at the wavelength of 1555 nm (spatial resolution is ≃500 m). The fiber loss at the wavelength of 1550 nm is 0.2 dB/km and it remains mostly flat from 1450 to 1620 nm. The nonlinear coefficient, measured with a Sagnac interferometric technique [17] was found to be $\gamma = 2.7$ W^{-1}km^{-1}. The Raman gain coefficient at the pump wavelength was measured by direct probing with a tuneable laser diode and the obtained result was $g_R = 1$ W^{-1}km^{-1}.

Figure 1 shows the output supercontinuum spectra at room temperature for different input powers, measured by means of an optical spectrum analyzer with 0.05 nm resolution. For low powers, the effect of modulational instability is clearly visible as two nearly symmetric noise side bands around the center frequency. The slight asymmetry between them is caused by Raman gain of the red-shifted and attenuation of the blue-shifted. **The wavelengths of the Stokes side are located in the same spectral region of the Raman amplification curve generated by the pump and the ones of the**

antiStokes side are in the Raman attenuation region [15]. Increasing the pump power, the MI gain grows, the power transfer from pump to the noise side bands is more rapid, and the asymmetry between the gain side bands becomes larger **because of Raman effect**. Beyond 1.5 W, complete pump depletion from pump to SC is achieved.

In our case, the changes in the SC spectrum with the fiber temperature might be caused by (i) a change in the value of the nonlinear coefficient; (ii) a change in the dispersion and (iii) a change in the Raman contribution to the fiber nonlinearity. A simple evaluation taking into account our temperature range (20-80C) allows us to discard this last cause as a source of important changes in the SC spectrum [18]. However, experimental measurements have shown that the nonlinear coefficient decreases strongly with temperature [19](-0.24%/C) while the zero-dispersion wavelength increases slightly [20] (+28 pm/C).

To test the temperature dependence of the generated SC we introduced the fiber into a stove with controlled temperature. A thermocouple was sticked to the inner side of the spool to measure the actual temperature of the fiber. To ensure thermal uniformity over the whole fiber, we performed our measurements only when the fiber and the environment had rested at the same temperature for more than one hour. We assess the corresponding changes in the fiber dispersion and nonlinear coefficient by measurement of the spontaneous MI side lobes appearing at each side of the pump at low powers ($\simeq$100 mW). From the well-known theory of modulational instability in optical fibers [21] we know that the maximum of the MI gain side lobes should appear at a certain frequency detuning from the pump frequency given by $\Omega_m = \sqrt{2\gamma P_0/|\beta_2|}$, γ being the nonlinear coefficient of the fiber and P_0 being the pump power. For this frequency detuning, the MI gain is given by $g_{max} = 2\gamma P_0$. Thus, keeping the power and the nonlinear coefficient constant, the variations in β_2 induce variations only on Ω_m, while the variations in γ induce variations both on g_{max} and Ω_m.

Figure 2 shows the MI side lobes for a pump power of ≃100 mW measured at different temperatures. We appreciate a certain decrease in the peak value of the MI side lobes as the temperature grows, meaning probably that the nonlinear coefficient has decreased, in agreement with the previous experimental results. Simultaneously we can appreciate that while the temperature increases, the maximum gain is produced for larger frequency detunings, thus meaning that the fiber dispersion is lower for higher temperatures, again in qualitative agreement with previous results. We check this agreement further by using the previous relation between Ω_m and β_2. Using the measured nonlinear coefficient at 20C (γ=2.7 $W^{-1}\cdot km^{-1}$), and taking into account the empirical temperature variation of the nonlinear coefficient (-0.24%/C), we estimate the dispersion coefficient for the different temperatures. At 20C the estimated dispersion coefficient is 0.072 $ps\cdot nm^{-1}\cdot km^{-1}$ and it decreases to 0.035 $ps\cdot nm^{-1}\cdot km^{-1}$ at 80C almost linearly. By a linear fitting of the results, we obtain a thermal variation coefficient of -0.0006 $(ps\cdot nm^{-1}\cdot km^{-1})$/C, which is in good agreement with the measurements reported elsewhere [20] for this kind of fibers. In turn, the measured variations of the MI side lobes agree well with the expected variations of g_{max} induced by the variations of γ with temperature. It is important to note that in all these estimations, we have averaged the values obtained for the right and left hand lobes, in order to eliminate the Raman asymmetry.

In figure 3 we show the SC spectra obtained for a pump power of 2.1 W at different temperatures. We can see a consistent growth of the 10-dB SC width with temperature. The widths at 20, 40, 60 and 80C are, respectively, 151 nm, 159 nm, 182 nm and 192 nm. The growth of the SC width with temperature is not linear, but it follows a clear increasing tendency. From 20 to 80C, the relative increase in the SC width is approximately 27%. This increase is associated with the broadening of the MI side lobes caused by the change in the fiber dispersion. Effectively, the MI process causes a rapid broadening of the pump spectrum. This causes a broadening of the Raman spectrum since it is built from the contributions of a broad range of wavelengths. It is also noticeable that pump depletion is more intense for lower temperatures. This is most probably related to the decrease in γ with temperature, which causes a slower power transfer from the pump to the MI side lobes.

3 Conclusion

To sum up, we have studied the effect of temperature variations on supercontinuum generation in optical fibers using a continuous-wave pump propagating in the region of small anomalous dispersion. We have shown that the temperature-induced changes in the fiber dispersion are responsible of a different behaviour in the MI-induced broadening of the pump spectrum. This, in turn, causes a different spectral distribution of the Raman-scattered light at the fiber output. We believe that working with shorter, uncoated fibers over a wider temperature range might provide a useful means of tuning the fiber dispersion and the width of the generated continuum in other setups using pulsed sources of high peak power.

4 Acknowledgments

We acknowledge fruitful discussions with Dr. Frederique Vanholsbeeck and Stephane Coen from the University of Auckland and Dr. Luc Thevenaz from EPFL in Lausanne, Switzerland. This work has been supported through projects TIC2000-2005, TIC 2003-01869 and CM 07T/004L/2003-1 and the program of grants I3P from the CSIC.

References

[1] S. A. Diddams, D. J. Jones, J. Ye, S. T. Cundiff, J. L. Hall, J. K. Ranka, R. S. Windeler, R. Holzwarth, T. Udem, and T. W. Hansch, Phys. Rev. Lett. **84** 5102-5105 (2000)

[2] D. J. Jones, S. A. Diddams, J. K. Ranka, A. Stentz, R. S. Windeler, J. L. Hall and S. T. Cundiff, Science. **288** 635-639 (2000)

[3] D. L. Marks, A. L. Oldenburg, J. J. Reynolds and S. A. Boppart, Opt. Lett., **27** 2010-2012 (2002)

[4] I. Hartl, X. Li, C. Chudoba, R. Ghanta, T. Ko, J. G. Fujimoto, J. K. Ranka and R. S. Windeler, Opt. Lett. **26** 608-610 (2001)

[5] T. Morioka, K. Mori and M. Saruwatari, Electron. Lett. **29** 862-864 (1993)

[6] H. Takara, T. Ohara and K. Sato, Electron. Lett. **39** 1078-1079 (2003)

[7] S. Coen, A. Hing Lun, R. Leonhardt, J. D. Harvey, J. C. Knight, W. J. Wadsworth and P. St. J. Russell, J. Opt. Soc. Am B **19** 753-763 (2002)

[8] T. A. Birks, W. J. Wadsworth and P. St. J. Russell, Opt. Lett. **25** 1415-1417 (2000)

[9] M. Prabhu, N. S. Kim and K. Ueda, Jpn. J. Appl. Phys. **39** L291-L294 (2000)

[10] J. W. Nicholson, A. K. Abeeluck, C. Headley, M. F. Yan and C. G. Jorgensen, Appl. Phys. B, **77** 211-218 (2003)

[11] M. Gonzalez-Herraez, S. Martin-Lopez, P. Corredera, M. L. Hernanz and P. R. Horche, Opt. Commun. **226** 323-328 (2003)

[12] A. V. Advokhin, S. V. Popov and J. R. Taylor, Opt. Lett. **28** 1353-1355 (2003)

[13] A. Sauter, S. Pitois, G. Millot and A. Picozzi, Opt. Lett. **30** 2143-2145 (2005)

[14] F. Vanholsbeeck, S. Martin-Lopez, M. Gonzalez-Herraez and S. Coen, Opt. Exp. **13** 6615-6625 (2005)

[15] A.K. Abeeluck and C. Hedley, Opt. Lett. (**30) 61-63 (2005)**

[16] M. Gonzalez-Herraez, L. Thevenaz and Ph. Robert, Opt. Lett. 28 2210-2212 (2003)

[17] D. Monzon-Hernandez, A. N. Starodumov, Yu. O. Barmenkov, I. Torres-Gomezand F. Mendoza-Santoyo, Opt. Lett. 23 1274-1276 (1998)

[18] S. A. E. Lewis, S. V. Chernikov and J. R. Taylor, Opt. Lett. 24 1823-1825 (1999)

[19] Y. Imai and K. Mizuta, Opt. Lett. 25 1412-1414 (2000)

[20] T. Kato, Y. Koyano and M. Nishimura, Opt. Lett. 25 1156-1158 (2000)

[21] G. P. Agrawal "Nonlinear Fiber Optics" (Academic Press, 1995), Chap. 5.

List of Figures

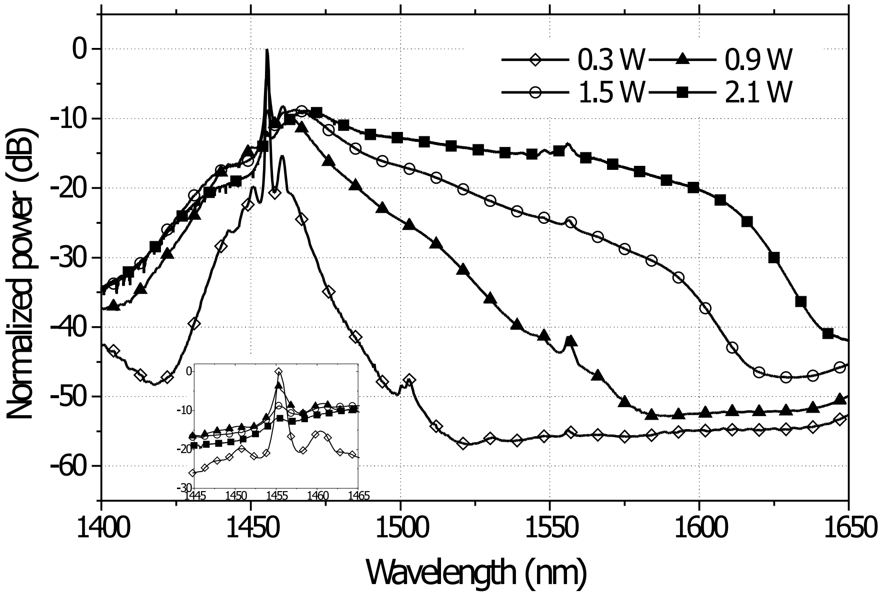

Figure 1. SC spectrum with different pump powers at room temperature (≃20C). All the curves have been normalized to the same peak value. Inset shows how increasing pump power leads to a more efficient pump depletion.

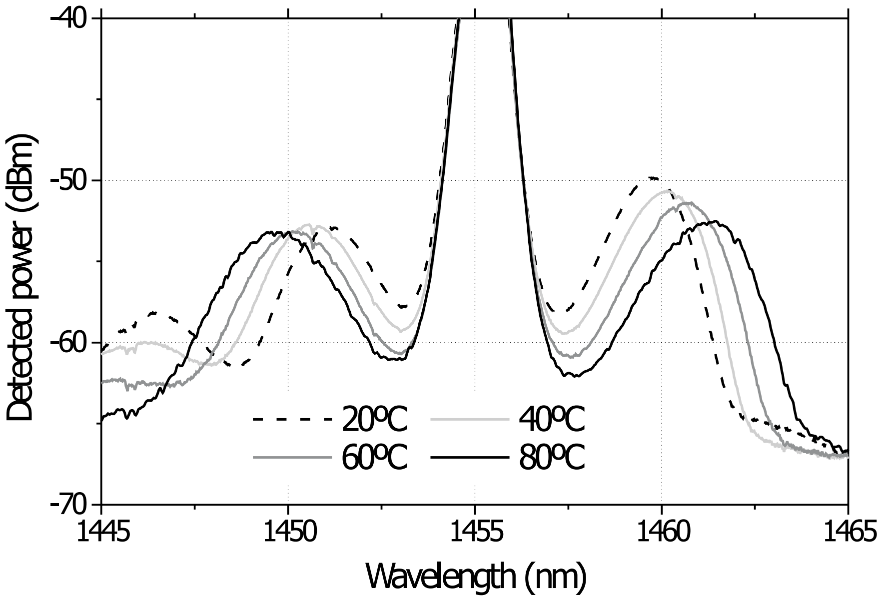

Figure 2. MI spectrum around the pump wavelength for different temperatures. As the temperature grows, the asymmetry between the MI side lobes is less evident.

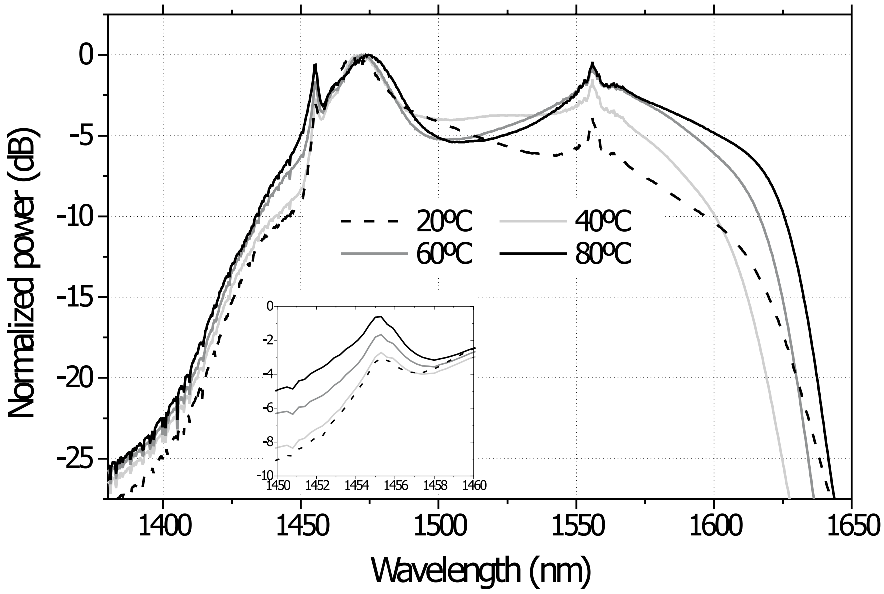

Figure 3. SC spectrum for different temperatures. The pump input power is always 2.1 W. Each curve has been normalized by its own maximum to show more clearly the increase of the SC width. The inset shows how pump depletion is less intense as the temperature grows.